



Influence of alkylene spacer length on photoinduced molecular reorientation and LC alignment behavior in photo-cross-linkable liquid crystalline polymeric films with H-bonded cinnamic acid side groups

Nobuhiro Kawatsuki*, Yusuke Koezuka

Department of Materials Science and Chemistry, Graduate School of Engineering, University of Hyogo, 2167 Shosha Himeji, Himeji, Hyogo 671-2280, Japan

ARTICLE INFO

Article history:

Received 3 February 2009

Received in revised form

19 March 2009

Accepted 22 March 2009

Available online 27 March 2009

Keywords:

Liquid crystalline polymer

Hydrogen bonds

Photoinduced orientation

ABSTRACT

Photoinduced reorientation of liquid crystalline polymethacrylates comprised of various lengths of alkylene spacers terminated with 4-oxycinnamic acid in the side chain and low-molecular liquid crystal (LC) alignment on the resultant photoreacted films were investigated using linearly polarized UV light. As the length of the spacer increased, the photoinduced optical anisotropy (ΔA) of the thin films increased, and ΔA increased as the irradiating temperature increased. Exposing the polymeric films in the LC temperature range of the material generated an in-plane molecular reorientation because the small photoinduced ΔA was simultaneously amplified. The low-molecular LCs aligned homogeneously on the photoreacted polymeric films, but the LC alignment direction depended on the alkylene spacer length and the degree of the photoreaction.

© 2009 Elsevier Ltd. All rights reserved.

1. Introduction

Irradiating photoreactive polymeric films, including azobenzene-containing polymers and photo-cross-linkable polymers comprised of cinnamate or coumarin moieties, with linearly polarized (LP) light induces optical anisotropy (ΔA) due to a polarization-axis-selective photoreaction [1,2]. A large ΔA is generated when a molecular reorientation is accompanied by an axis-selective photoreaction [3–7]. Numerous studies have investigated the photoinduced molecular reorientation of azobenzene-containing polymers based on an axis-selective *trans-cis-trans* photoisomerization of azobenzene molecules in both liquid crystalline (LC) and non-LC polymers, which are applicable to reversible optical memory and holographic devices [3,5–7]. For photo-cross-linkable polymeric films, exposure to LP ultraviolet (LPUV) light induces a small photoinduced ΔA due to axis-selective photo-cross-linking [2,4]. In addition, molecular reorientation can be thermally enhanced when the material exhibits LC characteristics [4,8–10]. These reoriented films are useful for the passive optical devices such as birefringent films and write-once optical and holographic memories because the reoriented structure is stabilized by the photo-cross-linking.

The photoinduced molecular reorientation is affected by the alkylene spacer length, which is covalently connected between the photosensitive side groups and polymer main chain to ease the molecular motion of the side groups. Several studies on the photoinduced molecular reorientation of azobenzene-containing polymeric films with different spacer lengths have been reported [11–14], and out-of-plane reorientation and in-plane reorientation have been observed with long alkylene spacers. For a photo-cross-linkable polymer system, we conducted systematic studies on the thermally enhanced molecular reorientation of polymethacrylates terminated with mesogenic cinnamate side groups, and investigated the influence of the alkylene spacer length between the methacrylate backbone and the photoreactive mesogenic side groups on the thermally enhanced photoinduced reorientation behavior [15,16]. Although the films have similar photoinduced ΔA 's regardless of the spacer length, the spacer length influences the thermally induced molecular reorientation direction. Recently, we have reported a new photo-addressable LC polymer system based on H-bonded photo-cross-linkable mesogenic side groups; a polymethacrylate comprised of a hexamethylene spacer group terminated with a 4-oxycinnamic acid (CA) in its side chain (**P6**) exhibits a large photoinduced molecular reorientation [17]. Due to the H-bonded CA groups, the polymer displays a nematic LC property and high photoreactivity. However, the influences of the alkylene spacer length between the polymethacrylate backbone

* Corresponding author. Tel.: +81 792 67 4885; fax: +81 792 67 4886.

E-mail address: kawatuki@eng.u-hyogo.ac.jp (N. Kawatsuki).

and the CA side groups on the photoinduced ΔA have yet to be explored.

An important application of anisotropically photoreacted films is a photoalignment film for low-molecular LCs [18–21]. Many photoreactive polymers have been utilized for LC photoalignment layers, and the LC alignment direction in several LC photoalignment materials can be controlled by adjusting the exposure doses, which offers easy patterning of the LC alignment [22–24]. Previously, we have reported that photoreacted **P6** film shows uniform low-molecular LC alignment control both perpendicular and parallel to the polarization (**E**) of LPUV light, depending on the exposure doses [17,25]. Since the uniform LC alignment is determined by the interaction between the LC molecules and the photoalignment layer, the alkylene spacer length should affect the LC alignment behavior.

Hence, the purposes of this paper are to investigate the influence of the alkylene spacer length on the photoinduced molecular reorientation behavior of polymethacrylate comprised of an alkylene spacer group terminated with CA moiety and to demonstrate low-molecular LC alignment on the resultant photoreacted films. Due to the H-bonded CA side groups, all the polymers exhibited nematic LC characteristics, and irradiating with LPUV light generated optically anisotropic films. Both molecular reorientation and LC alignment greatly depended on the alkylene spacer length.

2. Experimental

2.1. Materials

All starting materials were used as received from Tokyo Kasei Chemicals. Fig. 1 shows the synthetic route for the polymers. Methacrylate monomers and the corresponding polymers were synthesized using a procedure similar to that used to synthesize **P6** [17]. Characterization of the **P0**, **P2**, **P8**, **P10**, and **P12** and corresponding monomers are summarized in the Supporting information. Table 1 summarizes the thermal property of the monomers, molecular weight, as well as the thermal and spectroscopic properties of the polymers.

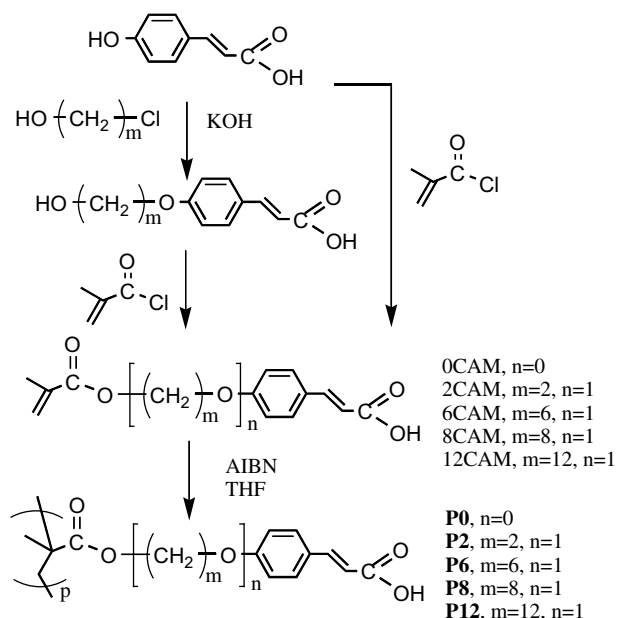


Fig. 1. Synthesis and chemical structure of **P0**–**P12** used in this study.

Table 1

Molecular weight and thermal property of the synthesized polymers.

Polymer	m	n	Molecular weight (g/mol) ^a		Thermal property ^b (°C)
			$M_n \times 10^{-4}$	M_w/M_n	
0CAM	–	0	–	–	C 170 N 190 I
2CAM	2	1	–	–	C 152 N 168 I
6CAM	6	1	–	–	C 118 N 127 I
8CAM	8	1	–	–	C 92 N 125 I
12CAM	12	1	–	–	C 90 N 125 I
P0	–	0	2.3	3.9	G 305 N (decomposed)
P2	2	1	1.2	3.6	G 170 N 220 I
P6	6	1	3.3	3.5	G 135 N 185 I
P8	8	1	2.8	3.9	G 140 N 189 I
P12	12	1	3.6	4.2	G 120 N 189 I

^a Molecular weight was determined using the methyl ester of the polymer. Measured with GPC, chloroform eluent, polystyrene standards.

^b C: crystalline, G: glass, N: nematic, I: isotropic. Determined by DSC and POM.

2.2. Photoreaction

Thin polymeric films, which were approximately 0.2 μm thick, were prepared by spin-coating a tetrahydrofuran (THF) solution of polymers (1.0 w/w%) onto quartz or KBr substrates. Photoreactions were performed using an ultrahigh-pressure Hg lamp equipped with Glan–Taylor polarizing prisms and a cut-filter under 290 nm to obtain LPUV light with an intensity of 10 mWcm⁻² at 365 nm. The degree of the photoreaction was estimated by monitoring the decrease in absorbance at 314 nm using UV spectroscopy.

2.3. Characterization

¹H NMR spectra using a Bruker DRX-500 FT-NMR and FTIR spectra (JASCO FTIR-410) confirmed the monomers and polymers. The molecular weight of the copolymer was measured after modifying the aromatic acid groups to the methyl ester by GPC (Tosoh HLC-8020 GPC system with Tosoh TSKgel column; eluent, chloroform) calibrated using polystyrene standards [25]. The thermal properties were examined using a polarization optical microscope (POM; Olympus BHA-P) equipped with a Linkam TH600PM heating and cooling stage and differential scanning calorimetry (DSC; Seiko-I SSC5200H) at a heating and cooling rate of 10 °C min⁻¹. The polarization absorption spectra were measured with a Hitachi U-3010 spectrometer equipped with Glan–Taylor polarization prisms. Temperature controlled FTIR spectra were recorded through a JASCO IRT-3000/FTIR-410 system with a Linkam TH600PM heating and cooling stage.

The photoinduced optical anisotropy, ΔA , which is expressed as Eq. (1), was evaluated using the polarization absorption spectra,

$$\Delta A = A_{\parallel} - A_{\perp} \quad (1)$$

where A_{\parallel} and A_{\perp} are the absorbances parallel and perpendicular to **E**, respectively. The absorbances were normalized using the one at 314 nm for the initial state. The in-plane order parameter, S , and the out-of-plane order parameter, Sh , are expressed in the form of Eqs. (2) and (3), respectively;

$$S = \frac{A_{\parallel} - A_{\perp}}{A_{(\text{large})} + 2A_{(\text{small})}} \quad (2)$$

$$Sh = 1 - \frac{A_{(\text{annealed})}}{A_{(\text{irradiated})}} \quad (3)$$

where A_{\parallel} and A_{\perp} are the absorbances parallel and perpendicular to **E**, respectively, and $A_{(\text{large})}$ is the larger value of A_{\parallel} and A_{\perp} , and $A_{(\text{small})}$ is the smaller one. $A_{(\text{annealed})}$ and $A_{(\text{irradiated})}$ are the average

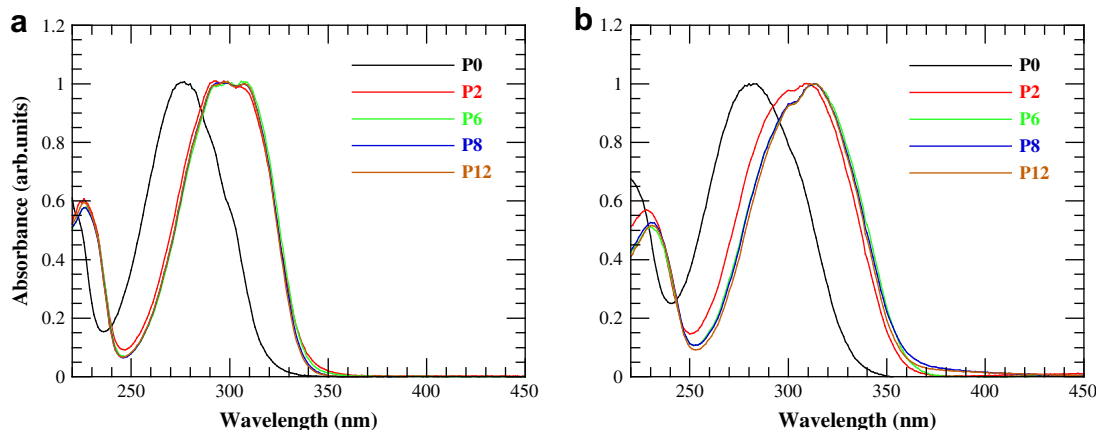


Fig. 2. UV absorption spectra of **P0–P12** (a) in THF solution and (b) films on quartz substrates.

absorbances of A_{\parallel} and A_{\perp} from the annealed film and the initial irradiated film, respectively. Additionally, this equation appropriately expresses the orientation order of the mesogenic groups in both directions.

2.4. Low-molecular LC alignment

A parallel LC cell was fabricated using two LPUV photoreacted polymeric films to evaluate the LC alignment behavior. The cell (12.5- μm thick) was filled with a nematic LC mixture (ZLI4792: Merck Japan, $T_i = 102\text{ }^{\circ}\text{C}$) doped with 0.1 wt% of disperse blue 14 (Aldrich Co.) at $110\text{ }^{\circ}\text{C}$ and then was slowly cooled. The homogeneous LC alignment direction and the orientational order of the DB14 were evaluated from a dichroic absorption measurement utilizing the guest-host effect.

3. Results and discussion

3.1. Synthesis, and thermal and spectroscopic properties of the polymers

Polymethacrylates with CA side groups were synthesized by solution radical polymerization from the corresponding

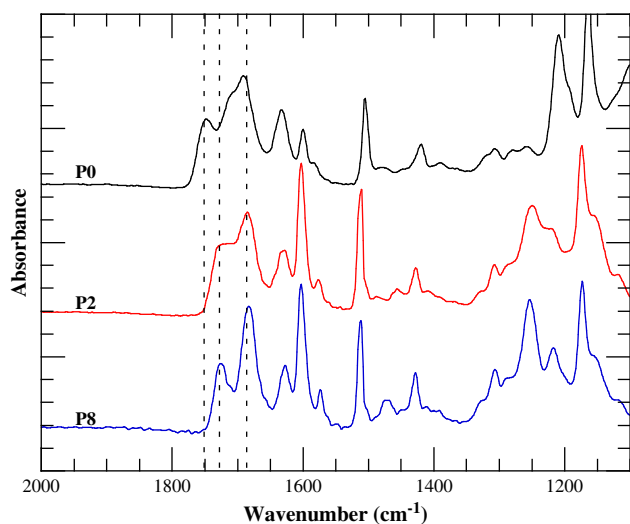


Fig. 3. FTIR spectra of **P0**, **P2** and **P8** films on CaF_2 substrates. Specific absorption bands are pointed with dotted lines.

monomers. All synthesized polymers were soluble in THF and DMF, but were insoluble in toluene and chloroform. Table 1 summarizes the molecular weights and thermal properties. All the monomers and polymers exhibited a nematic LC phase because the cinnamic acid side groups formed mesogenic H-bonded dimers [17,26–28]. **P0** revealed a LC phase in the high temperature range, which was accompanied by thermal decomposition. **P6**, **P8**, and **P12** showed a nematic LC phase in a similar temperature range, whereas **P2** had a higher LC temperature range.

Fig. 2a and b shows the UV absorption spectra of the polymers in THF solutions and films on quartz substrates, respectively. **P2**, **P6**, **P8**, and **P12** had similar absorption spectra, but **P0** absorbed at a shorter wavelength because CA was directly attached to the polymethacrylate main chain. In the films, the absorption maxima were red shifted due to the H-bonded structure of the CA side groups and partial aggregation. This red shift was smaller for the **P2** film than that for the **P6**, **P8**, and **P12** films. **P2** formed fewer H-bonded side groups as the solvent evaporated due to its short alkylene spacer.

IR spectroscopy was used to evaluate H-bonded formation, and Fig. 3 shows the FT-IR spectra of **P0**, **P2**, and **P8** films on CaF_2 substrates. The IR spectra of the **P6** and **P12** films were similar to **P8**. For **P2** and **P8**, the C=O stretching band of the polymethacrylate main chain was observed at 1725 cm^{-1} , but was at 1750 cm^{-1} for **P0** because methacrylate was directly attached to a phenyl group. For all the films, H-bonded C=O stretching of the CA groups was at 1685 cm^{-1} , but this absorption band for the **P0** and **P2** films was broader and weaker than that of **P8**. Additionally, when the **P2** and **P8** film was heated at $220\text{ }^{\circ}\text{C}$ and $200\text{ }^{\circ}\text{C}$ (isotropic temperature ranges), respectively, the absorbance of H-bonded C=O decreased and the absorbance around 1725 cm^{-1} increased due to the dissociation of the H-bondings. When the films were cooled to room temperature, the spectrum returned to the initial one for **P8**, while the absorption at 1685 cm^{-1} became sharper for **P2**, indicating the strong H-bond formation after heating (see Supporting information).

3.2. Photoreaction of the polymeric films with LPUV light

Polymeric films comprised of cinnamate or cinnamic acid groups photoreacted with LPUV light to induce films with a negative optical anisotropy ($\Delta A < 0$) due to the axis-selective photoreaction [2,4]. Fig. 4a and b plots the degree of the photoreaction (DP) of **P0–P12** films at room temperature and the resultant photoinduced ΔA values as a function of exposure doses, respectively. The **P2–P12** films had similar photoreactivities, but that of **P0** was

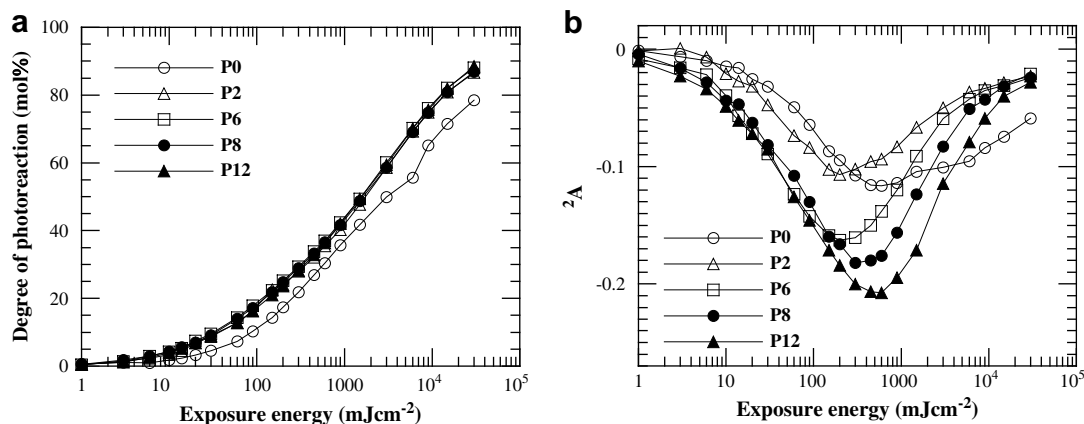


Fig. 4. (a) Degree of the photoreaction determined by monitoring the decrease in absorbance at 314 nm using UV spectroscopy, and (b) photoinduced optical anisotropy (ΔA) of the polymeric films which was normalized using the one at 314 nm for the initial state, as a function of exposure energy.

slightly slower. Despite similar photoreactivities, polymers with longer alkylene spacers generated larger ΔA values (Fig. 4b).

The axis-selective photoreaction was estimated by the polarization FTIR spectra. Fig. 5a and b shows the polarization FTIR spectra of **P2** and **P8** films when the DP was 28 mol%, respectively. For both films, negative ΔA 's at 1685 cm⁻¹, 1635 cm⁻¹ (C=C

stretching of CA), and 1600 cm⁻¹ (Ph-ring) were observed. The ΔA 's of these absorption bands in the **P8** film were greater than that of **P2**. Additionally, because ΔA at 1725 cm⁻¹ (C=O stretching of polymethacrylate) was negligible, the polymethacrylate main chain did not reorient upon the photoreaction. These results imply that in addition to the axis-selective photoreaction, a small photoinduced

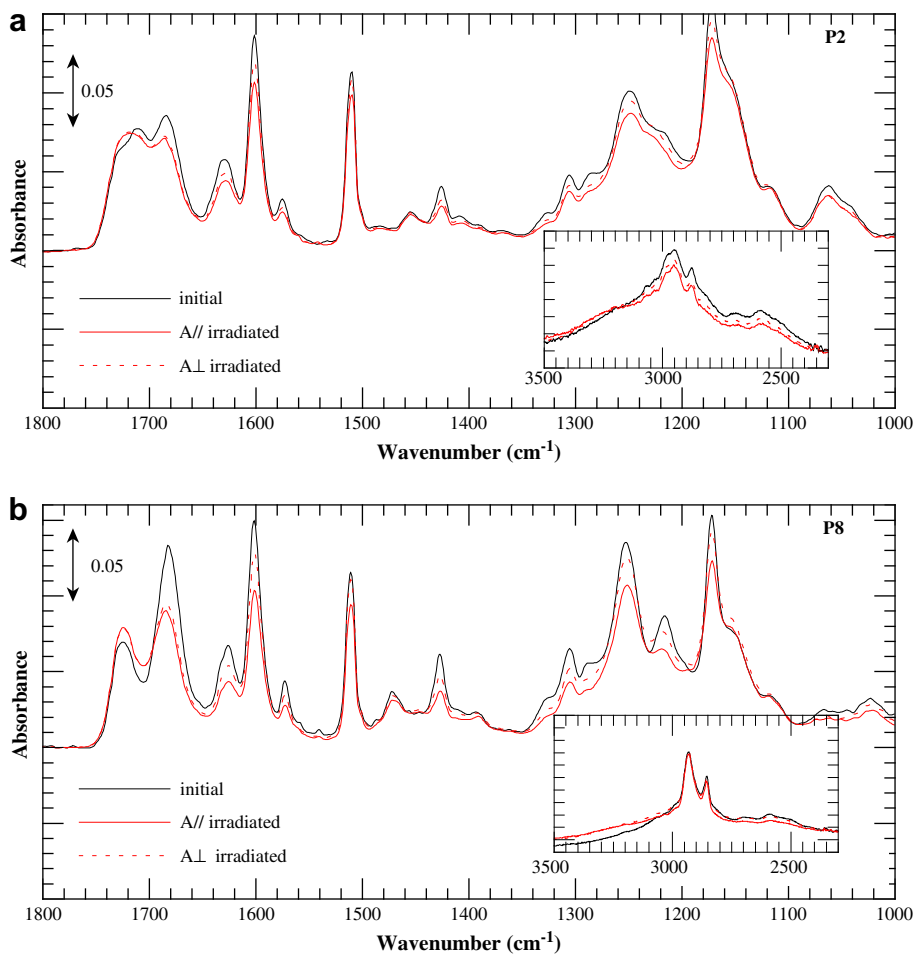


Fig. 5. FTIR spectra of (a) **P2** and (b) **P8** films on CaF₂ substrates before photoirradiating (black line) and after irradiating (red lines) for 600 mJ cm⁻² at 25 °C. A_{||} and A_⊥ are the solid lines and the dotted lines, respectively. Inset figure shows the absorption between 3500 and 2200 cm⁻¹. [For interpretation of the references to colour in this figure legend, the reader is referred to the web version of this article.]

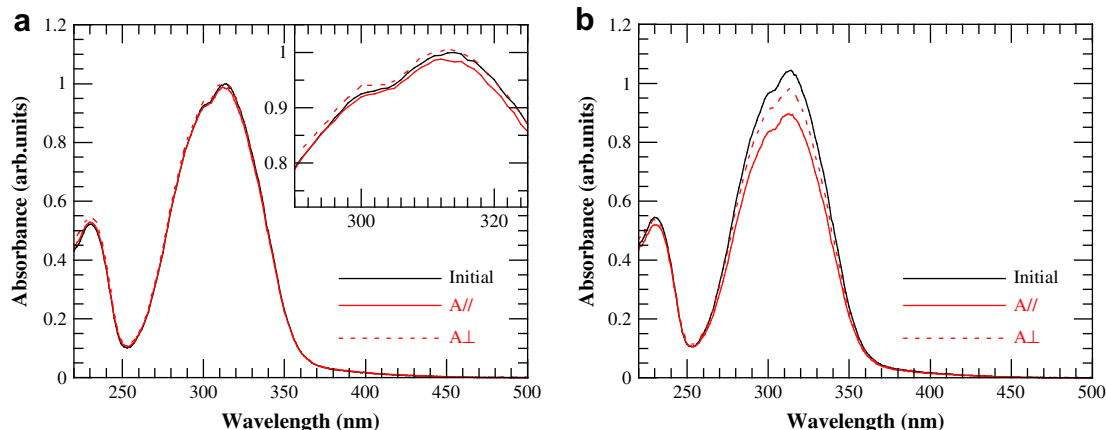


Fig. 6. UV-vis polarization spectrum of a **P8** film before photoirradiating, after irradiating with LPUV light at 70 °C. Solid line and dotted line represent A_{\parallel} and A_{\perp} , respectively. (a) Exposure energy; 3 mJ cm^{-2} , (b) Exposure energy; 20 mJ cm^{-2} .

molecular reorientation occurs when the alkylene spacer is long. The photoinduced molecular reorientation upon irradiating with LP light has been observed in azobenzene-containing polymeric films due to the axis-selective *trans-cis-trans* photoisomerization [3]. Similar phenomena will occur in CA containing polymers, but the contribution of this photoisomerization on the molecular reorientation was not evaluated because the photo-cross-linking reaction simultaneously occurred.

The molecular reorientation upon irradiating with LPUV light was directly estimated using the polarized UV absorption spectra at the early stage of the photoreaction. Fig. 6a plots the changes in the UV spectra of the **P8** film when the film was irradiated with 3 mJ cm^{-2} doses ($DP < 1 \text{ mol}\%$) at 70 °C, and reveals a small increase in the absorbance in the perpendicular direction after irradiating, suggesting a small molecular reorientation perpendicular to **E**. Further exposure showed an increase in ΔA , but the absorbances in both the parallel and perpendicular directions decreased because the [2 + 2] photodimerization reaction reduced the absorbances as shown in Fig. 6b. The **P6** and **P12** films also had a slight increase in the absorbances in the perpendicular direction at the early stage of the photoreaction, but **P0** and **P2** did not, indicating that molecular reorientation upon irradiating with LPUV light depends on the alkylene spacer length. Namely, a longer alkylene spacer increases the mobility of the photoinduced molecular reorientation.

Fig. 7a and b plots the maximum photoinduced ΔA values and the required exposure energy at the maximum absolute ΔA as a function of irradiation temperature, respectively. For **P0**, the photoinduced ΔA values were less than 0.11 regardless of the irradiation temperature due to its high T_g , but the other polymers were temperature dependent. In the lower irradiation temperature range ($T < T_g$, inset of Fig. 7a), ΔA was greater for longer alkylene spacers, and the photoinduced ΔA values slightly increased as the temperature increased when the required exposure energy was greater than 100 mJ cm^{-1} ($DP > 20 \text{ mol}\%$) (Fig. 7b). In these cases, the absorbances in both the perpendicular and parallel directions were smaller than that of the initial ones, indicating that the photoinduced ΔA is mainly generated by the axis-selective photoreaction of the CA groups as well as the small amount of the photoinduced molecular reorientation as described above. The increased mobility of the side groups for longer spacers and higher exposure temperatures resulted in a slight increase in the photoinduced molecular reorientation.

In contrast, when the irradiation temperature was in the LC temperature range of the polymer, larger maximum ΔA values were obtained with lower exposure energies ($DP < 10 \text{ mol}\%$, as shown in Fig. 7b). Additionally, the absorbance in the perpendicular direction greatly increased, suggesting that a large molecular reorientation perpendicular to **E**; molecular reorientation is the main reason for this large ΔA . Thermal amplification of the photoinduced ΔA has

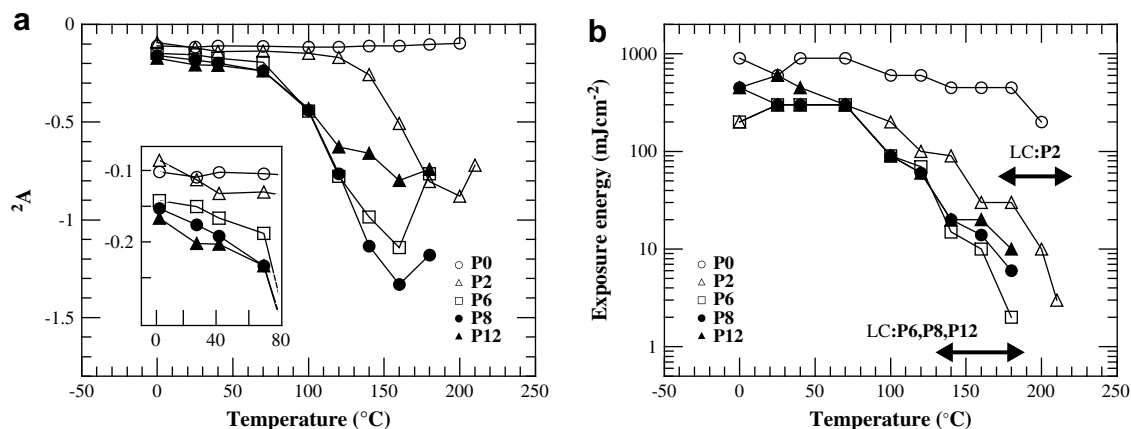


Fig. 7. (a) Maximum photoinduced optical anisotropy (ΔA) of the polymeric films upon exposure at various temperatures. Inset is an enlargement at low temperatures. (b) Required exposure energy when the maximum ΔA is obtained as a function of irradiating temperature, and arrows present the LC temperature range of the materials.

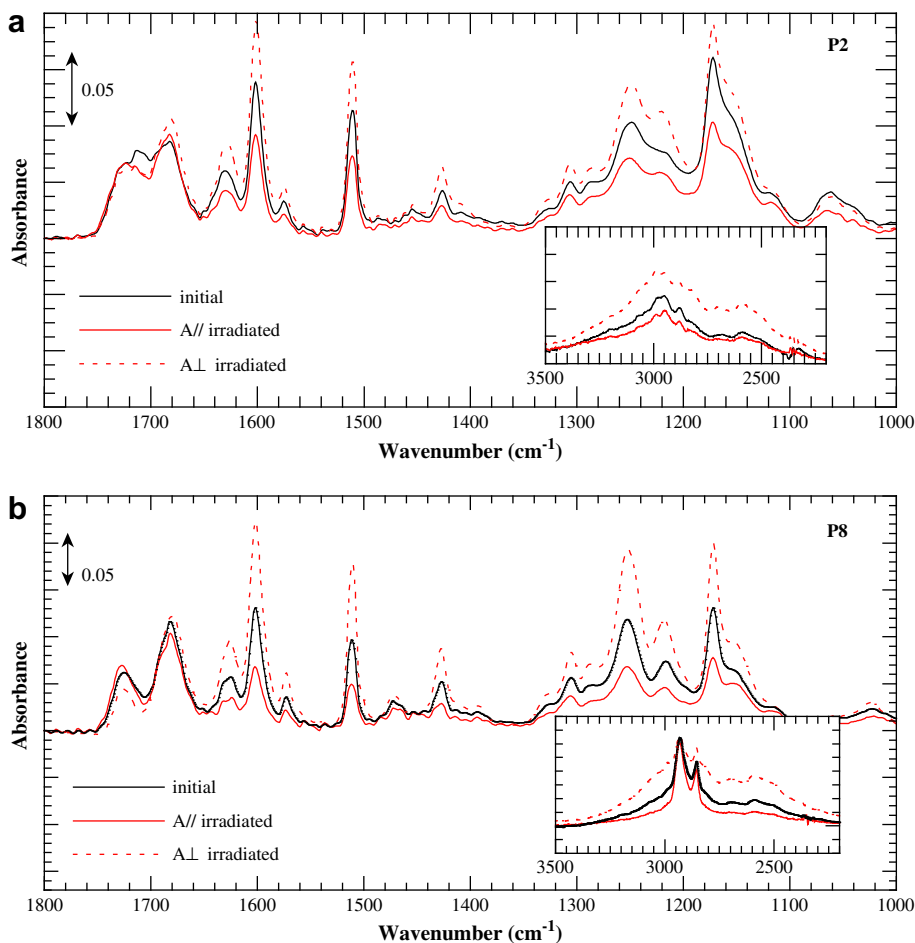


Fig. 8. FTIR spectra of (a) **P2** and (b) **P8** films on CaF_2 substrates before photoirradiating (black line) and after irradiating (red lines) for 10 mJ cm^{-2} at 190°C for **P2** and at 160°C for **P8**. Solid lines and dotted lines denote A_{\parallel} and A_{\perp} , respectively. [For interpretation of the references to colour in this figure legend, the reader is referred to the web version of this article.]

also been observed in other types of photo-cross-linkable LC polymers [4,8–10] and azobenzene-containing LC-polymers [3,29,30] when the films are exposed in the LC temperature range of the materials. Namely, a small photoinduced optical anisotropy was simultaneously enhanced due to the LC property of the mesogenic H-bonded CA side groups. Additionally, molecular reorientation of the mesogenic side groups followed the reorientation of the main chain.

Fig. 8a and b shows the polarization FTIR spectra of the **P2** and **P8** films before and after irradiating with LPUV light for 10 mJ cm^{-2} at 190°C and 160°C , respectively. In both cases, negative ΔA 's at $2800\text{--}2500 \text{ cm}^{-1}$, 1685 cm^{-1} , 1635 cm^{-1} , and 1600 cm^{-1} were observed, while ΔA at 1725 cm^{-1} became positive, suggesting that molecular reorientation of the side groups is accompanied by the reorientation of the methacrylate main chain parallel to **E** of LPUV light.

3.3. Thermal enhancement of the photoinduced optical anisotropy

Except for **P0**, the photoinduced optical anisotropy of the polymeric films at the early stage of the photoreaction at r.t. was thermally amplified to generate a uniaxially molecular-oriented film, but the orientational order depended on the alkylene spacer length. Table 2 summarizes the photoinduced and thermally enhanced in-plane order (S) values of the polymeric films. Fig. 9a

and b shows the changes in the polarization UV–vis spectra of **P2** and **P8** films irradiated with 10 mJ cm^{-2} doses of LPUV light at r.t., and subsequent annealing at 190°C for **P2** and 160°C for **P8**, respectively. Although the maximum reorientation order was greater than -0.6 for the **P6** and **P8** films, the enhanced S values for **P2** and **P12** were small. Additionally, the reoriented films were thermally stable up to $(T_i - 20)^\circ\text{C}$ of the material. A short alkylene spacer restricts the mobility of the side groups, but a longer alkylene spacer also inhibits the effective molecular reorientation. This tendency is similar to the case of the photoinduced ΔA values when the irradiating temperature is varied (Fig. 7). Although polymeric

Table 2
Photoinduced and thermally enhanced in-plane order (S) and out-of-plane order (Sh) of the polymeric films.

Polymer	Exposure energy (mJ/cm^2)	DP ^a (%)	Annealing temp. ($^\circ\text{C}$)	S		Sh
				Initial ^b	Annealed ^c	
P2	10	3.3	190	-0.010	-0.35	-0.077
P6	10	3.7	160	-0.012	-0.63	-0.108
P8	10	3.9	160	-0.012	-0.70	-0.149
P12	10	3.6	160	-0.013	-0.59	-0.113

^a Degree of photoreaction.

^b S values after exposure.

^c Annealed for 10 min.

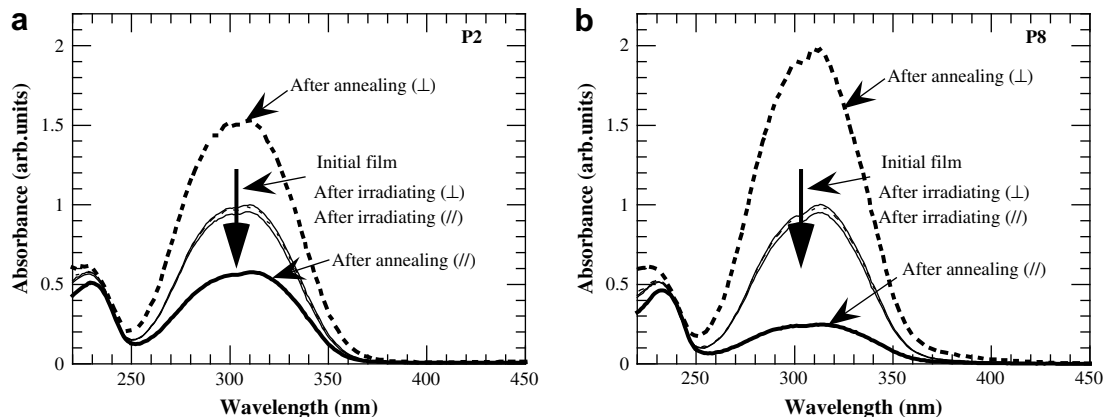


Fig. 9. UV-vis polarization spectrum of the polymeric films before photoirradiating, after irradiating with LPUV light (thin lines) for 10 mJ cm⁻² doses, and after subsequent annealing (thick lines) for 10 min. Solid lines and dotted lines represent A_{||} and A_⊥, respectively. (a) **P2**: Annealed at 190 °C. (b) **P8**: Annealed at 160 °C.

films with long alkylene spacers often display thermally induced out-of-plane reorientation [11–13], thermally induced out-of-plane reorientation was not generated regardless of the spacer length because the *Sh* values was lower than zero (Table 2).

Furthermore, the influence of the DP on the thermally enhanced molecular reorientation behavior was evaluated. Fig. 10 plots the photoinduced and thermally enhanced ΔA values as a function of the DP. The maximum thermally enhanced reorientation perpendicular to **E** of LPUV light was obtained when the DP was 2–6 mol%. In contrast, the molecular reorientation direction reversed, and became parallel to **E** of LPUV light ($\Delta A > 0$) when the DP was around 12 mol% because the [2 + 2] photo-cycloaddition products parallel to **E** of LPUV light acted as photo-cross-linked anchors for the molecular reorientation parallel to **E** of LPUV light [8–10,17]. The generated positive ΔA values were up to +0.33 for **P6**, +0.31 for **P8** and +0.15 for **P12**, while the thermally enhanced ΔA values for **P2** were less than +0.01 due to molecular mobility restrictions. As the DP further increased, the ΔA values after annealing decreased; the ΔA values after annealing remained slightly positive for the **P2** films, but those for **P6**, **P8**, and **P12** became negative again and approached the initial value after irradiating, especially for **P12**.

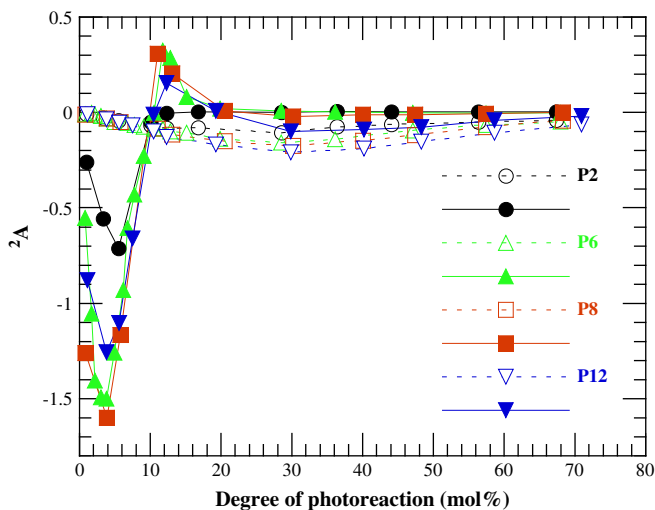


Fig. 10. Photoinduced and thermally enhanced ΔA values at 314 nm of **P2–P12** films as a function of DP. Open points are ΔA after exposure and closed points are after subsequent annealing. **P2**: Annealed at 190 °C, **P6–P12**: Annealed at 160 °C.

This indicates that many of the photoreacted products still act as photo-cross-linked anchors when the length of the alkylene spacer is short, and the reorientational ability parallel to **E** is lower when the alkylene spacer is long.

3.4. LC alignment

The reoriented polymeric films were applicable to the alignment layer for low-molecular LCs. We have previously demonstrated that a **P6** film exhibits uniaxial LC alignment ability where the LC alignment direction greatly depends on the DP [17,25]. Fig. 11 shows the LC alignment direction using two corresponding **P2**, **P6**, **P8**, and **P12** photoalignment films as a function of the DP. When LC molecules were aligned homogeneously, the order parameter of the dichroic dye (DB14) at 653 nm was around 0.4 in all cases, and disclinations were not observed in the LC cell.

For **P6**, **P8**, and **P12**, when the DP was between 1 and 7 mol%, which is where the H-bonded mesogenic groups of the polymeric films effectively reoriented perpendicular to **E** of LPUV light, the LCs aligned perpendicular to **E**. In these cases, the interaction between the LC molecules and the effectively reoriented H-bonded mesogenic groups perpendicular to **E** induced LC alignment along them [17]. For **P2**, LCs aligned perpendicular to **E** when the DP was between 1 and 3 mol%, but LCs randomly aligned when the DP was 3–13 mol%. In this case, azimuthal anchoring between the partially

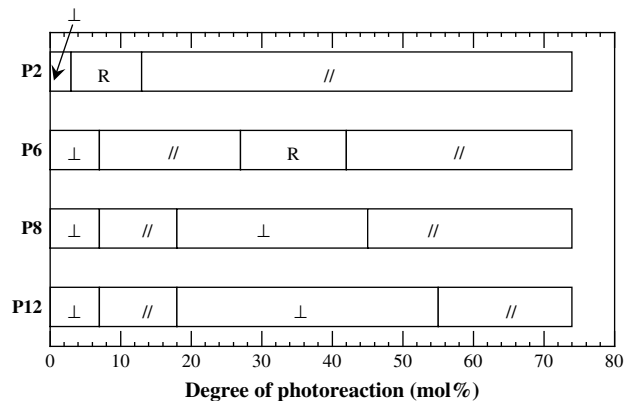


Fig. 11. LC alignment direction in the LC cell using two corresponding photoaligning films as a function of DP. \perp : LC alignment perpendicular to **E** of LPUV light. \parallel : LC alignment parallel to **E** of LPUV light. R: random LC alignment.

reoriented H-bonded mesogenic groups perpendicular to **E** and the photoreacted products parallel to **E** were comparable, which generated random LC alignment, although the molecular reoriented direction was perpendicular to **E**.

As the DP proceeded, the alignment direction changed and became parallel to **E** in all cases. This parallel LC alignment was observed when the DP was between 7 and 9 mol% for **P6**, **P8**, and **P12**, but the reorientation direction of the photoalignment layer remained perpendicular to **E**. This observation is attributed to the larger azimuthal anchoring of the photoreacted H-bonded CA side groups parallel to **E** rather than the partially reoriented H-bonded CA side groups perpendicular to **E** [17]. As the DP further increased (the DP is ~27 mol% for **P6**, ~18 mol% for **P8** and **P12**), a parallel LC alignment occurred when the reorientation direction of the photoalignment layer was parallel to **E** due to the strong interaction between the LC molecules as well as the

However, LCs, which randomly aligned for **P6** when the DP was approximately 28–37 mol%, aligned parallel to **E** upon further increasing the DP. In contrast, for **P8** and **P12**, LCs initially aligned perpendicular to **E** when the DP was greater than 18 mol%, and aligned parallel to **E** again upon further increasing the DP (DP > 45 mol% for **P8** and DP > 55 mol% for **P12**), similar to **P6**. Unlike these polymers, the LC alignment direction on the **P2** films was parallel to **E** when the DP was greater than 13 mol%.

For all the polymeric films in these DP ranges, molecular reorientation did not dominate. The high content of the photo-cross-linked H-bonded CA–CA groups and the small amount of molecular reorientation parallel to **E** caused parallel LC alignment, but for **P6**, a random LC alignment also appeared when azimuthal anchorings between the parallel and perpendicular directions of the photoalignment layer were competing. However, for **P8** and **P12**, azimuthal anchoring perpendicular to **E** was larger and there was an insufficient amount of photo-cross-linked H-bonded CA–CA groups. Namely, the long alkylene spacers reduced the azimuthal anchoring of the photo-cross-linked CA–CA side groups parallel to **E**. Therefore, perpendicular LC alignment was observed in **P8** and **P12** films, while random and parallel LC alignments were detected in **P6**. In all the case, greater amount of photoproducts generated the parallel LC alignment. These results agree with the findings that molecular reorientation of the polymeric films is more difficult in the high DP range as the alkylene spacer length increased (Section 3.3).

4. Conclusion

The influence of the alkylene spacer length on the photoinduced molecular reorientation of liquid crystalline polymethacrylates comprised of various lengths of alkylene spacers terminated with 4-oxycinnamic acid in the side chain as well as LC alignment on the resultant films was investigated. A longer alkylene spacer resulted in a greater photoinduced optical anisotropy. Except for **P0**, thermal amplification of the photoinduced ΔA was generated in the early stage of the photoreaction. All polymeric films produced a homogeneous LC alignment, which could control the alignment direction by adjusting the exposure doses. These reoriented films should be applicable to birefringent films as well as the LC alignment layer for liquid crystal displays.

Acknowledgments

This work was partly supported by a Grant-in-Aid for Scientific Research (S, No.16105004) by the Japan Society for the Promotion of Science.

Appendix. Supplementary material

Supplementary material can be found, in the online version, at doi:10.1016/j.polymer.2009.03.033.

References

- [1] (a) Weisner U, Reynolds N, Boeffel C, Spieses HW. *Makromol Chem Rapid Commun* 1991;12:457–64; (b) Shi Y, Steier WH, Yu L, Chen M, Dalton LR. *Appl Phys Lett* 1991;59:2935–7; (c) Natansohn A, Rochon P, Gosselin J, Xie S. *Macromolecules* 1992;25:2268–73.
- [2] Barachevsky VA. *Proc SPIE* 1991;1559:184–93.
- [3] (a) Ichimura K. *Chem Rev* 2000;100:1847–73; (b) Natansohn A, Rochon P. *Chem Rev* 2002;102:4139–76; (c) Ikeda T. *J Mater Chem* 2003;13:2037–57.
- [4] Kawatsuki N, Ono H. In: Nalwa HS, editor. *Organic electronics and photonics*, vol. 2. Stevenson Ranch, CA: American Scientific Publishers; 2007. p. 301–44.
- [5] Anderle K, Birenheide R, Eich M, Wendrorff JH. *Makromol Chem Rapid Commun* 1989;10:477–83.
- [6] (a) Date RW, Fawcett AH, Geue T, Haferkorn J, Malcolm RK, Stumpe J. *Macromolecules* 1998;31:4935–49; (b) Rutloh M, Stumpe J, Stachanov L, Kostromin S, Shibaev V. *Mol Cryst Liq Cryst* 2000;352:149–57.
- [7] Rodríguez FJ, Sánchez C, Villacampa B, Alcalá R, Cases R, Millaruelo M, et al. *Polymer* 2004;45:2341–8.
- [8] Kawatsuki N, Takatsuka H, Yamamoto T, Sengen O. *J Polym Sci Part A Polym Chem* 1998;36:1521–6.
- [9] Kawatsuki N, Suehiro C, Yamamoto T. *Macromolecules* 1998;31:5984–90.
- [10] Kawatsuki N, Goto K, Kawakami T, Yamamoto T. *Macromolecules* 2002;35:706–13.
- [11] Wu Y, Demachi Y, Tsutsumi O, Kanazawa A, Shiono T, Ikeda T. *Macromolecules* 1998;31:1104–8.
- [12] Han M, Ichimura K. *Macromolecules* 2001;34:82–9.
- [13] Han M, Morino S, Ichimura K. *Macromolecules* 2000;33:6360–70.
- [14] Uchida E, Shiraku T, Ono H, Kawatsuki N. *Macromolecules* 2004;37:5282–91.
- [15] Kawatsuki N, Hayashi M, Yamamoto T. *Mol Cryst Liq Cryst* 2001;368:423–30.
- [16] Kawatsuki N, Hayashi M, Yamamoto T. *Macromol Chem Phys* 2001;202:3087–98.
- [17] Uchida E, Kawatsuki N. *Macromolecules* 2006;39:9357–64.
- [18] O'Neill M, Kelly SM. *J Phys D: Appl Phys* 2000;33:R67–84.
- [19] Schadt M, Schmitt K, Kozinkov V, Chigrinov V. *Jpn J Appl Phys* 1992;31:2155–64.
- [20] Schadt M, Seiberle H, Schuster A. *Nature* 1994;381:212–5.
- [21] Gibbons WM, Kosa T, Palffy-Muhoray P, Shannon PJ, Sun ST. *Nature* 1995:43–6.
- [22] (a) Kawatsuki N, Ono H, Takatsuka H, Yamamoto T, Sengen O. *Macromolecules* 1997;30:6680–2; (b) Kawatsuki N, Matsuyoshi K, Hayashi M, Takatsuka H, Yamamoto T. *Chem Mater* 2000;12:1549–55.
- [23] Trajakovska A, Kim C, Marshall KL, Mourey T, Chen SH. *Macromolecules* 2006;39:6983–9.
- [24] Jackson PO, O'Neill M, Duffy WL, Hindmarsh PH, Kelly SM, Owen GJ. *Chem Mater* 2001;13:694–703.
- [25] Kawatsuki N, Kawanishi T, Uchida E. *Macromolecules* 2008;41:4642–50.
- [26] Praefcke K, Kohne B, Gündogân B. *Mol Cryst Liq Cryst Lett* 1990;7:27–32.
- [27] (a) Lin HC, Hendrianto J. *Polymer* 2005;46:12146–57; (b) Shandryuk GA, Kuptsov SA, Shatalova AM, Plate NA, Talroze RV. *Macromolecules* 2003;26:3417–23.
- [28] (a) Kato T, Fréchet JM. *Macromolecules* 1989;22:3818–9; (b) Kato T, Fréchet JM. *J Am Chem Soc* 1989;111:8533–4; (c) Kato T, Mizoshita N, Kanie K. *Makromol Rapid Commun* 2001;22:797–814; (d) Kato T, Mizoshita N, Kishimoto K. *Angew Chem* 2006;45:38–68.
- [29] Kidowaki M, Fujiwara T, Morino S, Ichimura K, Stumpe J. *Appl Phys Lett* 2000;76:1377–9.
- [30] Wu Y, Zhang Q, Kanazawa A, Shiono T, Ikeda T, Nagase Y. *Macromolecules* 1999;32:3951–6.